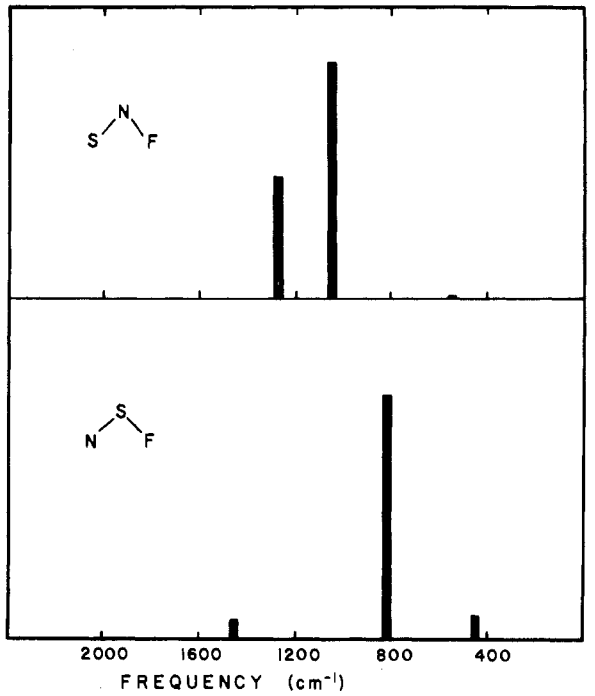

Figure 2. Computed IR spectra (6-31G*) of NSF and SNF. Intensities are relative to the strongest band in NSF at 814 cm^{-1}.

reached. Namely, the conversion of SNF to NSF was estimated to have an activation barrier of only 8.6 kcal/mol. This would preclude the isolation of SNF at room temperature. However, our results with correlation (6-31G*/MP2) give an activation energy of 33.4 kcal/mol for this isomerization, which suggests that SNF should be isolable at or near room temperature.

In Table IV the IR frequencies for both NSF and SNF are given along with predicted intensities. A comparison of the 6-31G* calculated frequencies with experimental frequencies[24] for NSF indicates quite reasonable agreement, although all frequencies are calculated to be too high as we have earlier found[25] with the 6-31G* basis set. No quantitative data are available for the intensities of the IR bands of NSF. Inclusion of correlation (6-31G*/MP2) is seen to improve greatly the agreement between theory and experiment for two of the three bands. However, for the N–S stretch agreement is worse at this level, with this band calculated to be at even higher frequency than with the 6-31G* wave function. We have noted similar erratic behavior of the calculated frequency of the C–S stretch in thirene as the basis set is changed.[28] On the other hand, for SNF we find the anticipated decrease in frequencies on going from the 6-31G* to the 6-31G*/MP2 basis set. The 6-31G* spectra of NSF and SNF are shown in Figure 2, and it is seen that they are quite different.

In conclusion, it is found that although SNF has a higher energy minimum than NSF, the isomerization from SNF to NSF has a sufficiently high activation energy to make SNF experimentally accessible and that the IR spectra of the two are sufficiently different to allow easy identification of the yet unknown SNF.

Registry No. NSF, 18820-63-8; SNF, 13537-38-7.

(24) Shimanouchi, T. *J. Phys. Chem. Ref. Data* **1977**, *6*, 993.
(25) Hess, B. A., Jr.; Čársky, P.; Schaad, L. J. *J. Am. Chem. Soc.* **1983**, *105*, 695.
(26) We have used the values of the fundamental constants recommended by: Cohen, E. R.; Taylor, B. N. *J. Phys. Chem. Ref. Data* **1973**, *2*, 663. With these values, 1 hartree = 627.5092 kcal/mol and 1 bohr = 0.5291 7706 Å.
(27) Mirri, A. M.; Guarnier, A. *Spectrochim. Acta* **1967**, *23*, 2159.
(28) Allen, W.; Schaad, L. J.; Hess, B. A., Jr., unpublished results.

Contribution from the Chemistry Division,
Los Alamos National Laboratory, Los Alamos, New Mexico 87545

Desolvation Method for Assessment of Crystallization Energies and Ion Crowding in Rare-Earth Perchlorates, Chlorides, and Nitrates

E. I. ONSTOTT,* LAURA B. BROWN, and E. J. PETERSON*

Received December 5, 1983

Gibbs energy changes on removal of solvent water to crystallize rare-earth perchlorates, chlorides, and nitrates from saturated solutions have been computed from activity data in the literature. These values are combined with heat of dilution data to give second-law entropy changes. Perchlorates and chlorides require about the same Gibbs energy change for crystal formation, although the saturated solution compositions are considerably different. Nitrates require about half of the Gibbs energy change required for perchlorates and chlorides. The work requirement for crystallization of $[Pr_2Cl_2(H_2O)_{14}]Cl_4$ is 500 cal mol^{-1} less than for $[NdCl_2(H_2O)_6]_2Cl_2$. Exothermic heat results from crystallization of the former compound, while heat absorption results from crystallization of the latter. All nitrates evolve heat on crystallizing. Second-law values of $T\Delta S$ show that the cation-stabilization energy of $[Pr_2Cl_2(H_2O)_{14}]Cl_4$ vs. $[PrCl_2(H_2O)_6]_2Cl_2$ is 150 cal mol^{-1}. Entropy changes on crystallization are positive only for perchlorates with atomic numbers larger than that of dysprosium. This behavior is interpreted to indicate a nearly perfect fit of ions and water at dysprosium, with cation crowding at smaller rare-earth atomic numbers and anion crowding at larger atomic numbers. Other ion-crowding effects are discussed. Extrapolations and interpolations for promethium show pivotal behavior that can be resolved when saturated-solution data become available.

Introduction

Many of the reported thermochemical cycles for hydrogen production by water splitting incorporate a step for removal of solvent water to produce a crystalline product for recycle.[1-7] There is a need for rigorous evaluation of work and heat requirements for crystal formation based on properties of the

(1) Sato, S.; Shimizu, S.; Nakajimia, H.; Onuki, K.; Ikezoe, Y.; Surva, T. "Hydrogen Energy Progress"; Veziroglu, T. N., Van Vorst, W. D., Kelley, J. H., Eds.; Pergamon Press: New York, 1982; Vol. IV, p 533.
(2) Remick, R.; Carty, R.; Sammells, A. Reference 1, p 567.
(3) Jones, W. M. Reference 1, p 591.
(4) Mason, C. F. V.; Bowman, M. G. Reference 1, p 665.
(5) Bamberger, C. E.; Nichols, D. H. *Int. J. Hydrogen Energy* **1979**, *4*, 517.
(6) Appleman, E. H.; Basile, L. J.; Richards, R. R.; Schreiner, F. *Int. J. Hydrogen Energy* **1981**, *6*, 267.

0020-1669/84/1323-2430$01.50/0

solutions and crystals. In this paper we quantify desolvation energies of saturated solutions of rare-earth perchlorates, chlorides, and nitrates. Work of desolvation values are combined with heat of dilution data to give second-law entropy changes. The rare-earth series is ideally suited for finding effects of cation size and cation hydration on energy requirements.

The precision of the work of Spedding and co-workers on the properties of concentrated rare-earth electrolytes and crystal hydrates is well-known. Their publications are the source of most of the data used in this paper. Specific references are cited.

Recently Pitzer, Peterson, and Silvester gave a theoretical treatment of the thermodynamic properties of rare-earth chloride, nitrate, and perchlorate electrolytes,[8] but they did not consider phase-transfer chemistry.

Mechanisms

When 1 mol of water is removed by vaporization from a dilute solution containing 1 mol of rare-earth(III) salt, the ratio of H_2O/RE in the solution decreases by 1. Continued removal of water results in formation of a saturated solution with a fixed H_2O/RE ratio. The crystal hydrate that precipitates at equilibrium also has a fixed ratio of H_2O/RE. For removal of 1 mol of water at equilibrium, the division of remaining H_2O between phases is

$$X(\text{cryst } H_2O/RE) + (1 - X)(\text{satd } H_2O/RE) = (\text{starting } H_2O/RE) - 1$$

where X is the mole fraction of rare earth in the crystal phase. Because the starting ratio of H_2O/RE is also the saturation ratio

$$1/X = (\text{satd } H_2O/RE) - (\text{cryst } H_2O/RE) \quad (1)$$

All the rare earth will be in the crystal hydrate when all the nonhydrate solvent water is removed. Further, since the saturated electrolyte composition is fixed, the work of removing the last solvent water will be the same as the work of removing the first. The total isothermal work of removing all the nonhydrate solvent water and condensing it as pure water represents the work or Gibbs energy change for crystallizing 1 mol of crystal hydrate from saturated solution. Each rare earth will have a different crystallization ΔG. This Gibbs energy change is stored as chemical potential in the crystal hydrate and in the pure solvent water and can be retrieved, according to the second law, by simply adding the pure condensed water to the crystal hydrate.

Rare-earth chlorides, perchlorates, and nitrates are different in their requirements for hydrate water. Perchlorate anion may be too large to compete for cation inner-sphere water, and all eight waters of hydration present in crystalline rare-earth perchlorates are presumed to be inner-sphere bonded.[9] One oxygen of one perchlorate may also occupy an inner-sphere site.[10] However, X-ray confirmations are completely lacking. All rare-earth chloride crystal hydrates contain inner-sphere-bonded chloride ligands. Lanthanum, cerium, and praseodymium crystal cations are dimeric with 2 bridged chlorides, 14 cation waters, and no lattice waters.[11,12] The remaining rare-earth and yttrium chlorides have dimeric crystal cations, but each cation has two inner-sphere chlorides and six inner-sphere waters, and the dimer is loosely bonded through the hydrate structure. There is no lattice water.[13-15] Praseodymium chloride is a pivotal rare earth for crystal transformation, since it converts from the stable bridged dimer, $[Pr_2Cl_2(H_2O)_{14}^{4+}]$, to the $[PrCl_2(H_2O)_6^+]_2$ dimer simply by removal of two inner-sphere waters that are the most loosely bonded.[16] There is a change in the crystal cation coordination number from 9 to 8, which requires chloride migration and cessation of chloride bridge bonding.

Crystal structure determinations have been reported for lanthanum, cerium, and praseodymium nitrates.[17-20] All are 6-hydrates with three nitrates inner-sphere bonded at six coordinate positions. In lanthanum and cerium, five waters are inner-sphere and one is in a lattice site, but praseodymium again shows pivotal cation size with four inner-sphere waters and two lattice waters. Neodymium through erbium form 6-hydrate nitrates that are stable at 295 K,[21] and these should be isostructural with $[Pr(NO_3)_3(H_2O)_4]\cdot 2H_2O$. The stable form of lutetium nitrate at 298 K is the 5-hydrate,[21] but there is no published crystal information for determining inner-sphere bonding.

Crystallization involves an enthalpy change also, which is the heat absorbed or evolved in the exact mechanism described above. Measurement of this enthalpy change is experimentally difficult, but the reverse procedure of dissolving the crystal in pure water and measuring the heat is the conventional method. Data are available for heats of solution of crystals to a definite molality, and data are reported also for heats of dilution of saturated electrolytes to nearly the same molality.[9,16,21-23]

The entropy changes for crystallization are given by the second law, and many geometric aspects of the rare-earth series can be interpreted.

Computations

For each mole of solvent water that is vaporized from the saturated solution and condensed as pure water, the work is

$$\Delta G = -RT \ln (A_e/A_1) \quad (2)$$

where A_e is the water activity of the electrolyte at saturation and $A_1 = 1$ for the activity of pure liquid water. The Gibbs energy of crystallization is

$$\Delta G_c = -X^{-1}RT \ln (A_e/A_1) \quad (3)$$

where ΔG_c is the work of formation of 1 mol of RE crystal hydrate from saturated solution and X is the mole fraction of rare earth precipitated for each mole of solvent water vaporized.

The enthalpy of crystallization is the thermodynamic inverse of the enthalpy change on dissolving 1 mol of rare-earth hydrate in exactly the right amount of water to form 1 mol of saturated solution at the specified temperature:

$$\Delta H_c = -\Delta H_{sat} \quad (4)$$

The saturation ΔH is the difference between the heat of solution of the crystal hydrate at some value of molality (which is less than the saturation molality) and the heat of dilution of the saturated solution to the same value of molality. The reference of infinite dilution also can be used.

(7) Peterson, E. J.; Onstott, E. I.; Bowman, M. G. "The Rare Earths in Modern Science and Technology"; McCarthy, G. J., Rhyne, J. J., Eds.; Plenum Press: New York, 1978; p 245.
(8) Pitzer, K. S.; Peterson, J. R.; Silvester, L. F. *J. Solution Chem.* **1978**, *7*, 45.
(9) Spedding, F. H.; Mohs, M. A.; Derer, J. L.; Habenschuss, A. *J. Chem. Eng. Data* **1977**, *22*, 142.
(10) Bunzli, J. G.; Yersin, J. R.; Mabillard, C. *Inorg. Chem.* **1982**, *21*, 1471.
(11) Habenschuss, A.; Spedding, F. H. *Cryst. Struct. Commun.* **1978**, *7*, 535; *Ibid.* **1979**, *8*, 511.
(12) Peterson, E. J.; Onstott, E. I.; Von Dreele, R. B. *Acta Crystallogr., Sect. B* **1979**, *B35*, 805.
(13) Marezio, M.; Plettinger, H. A.; Zachariasen, W. H. *Acta Crystallogr.* **1961**, *14*, 234.
(14) Habenschuss, A.; Spedding, R. H. *Cryst. Struct. Commun.* **1980**, *9*, 71; *Ibid.* **1980**, *9*, 157, 207, 213.
(15) Bel'skii, N. K.; Struchkov, Y. T. *Sov. Phys.—Crystallogr.* (*Engl. Transl.*) **1965**, *10*, 15.
(16) Spedding, F. H.; Flynn, J. P. *J. Am. Chem. Soc.* **1954**, *76*, 1474.
(17) Fuller, C. C.; Jacobson, R. A. *Cryst. Struct. Commun.* **1976**, *5*, 349.
(18) Erickson, B.; Larsson, L. O.; Niinisto, L. *J. Chem. Soc., Chem. Commun.* **1978**, 616.
(19) Milinski, N.; Ribar, B.; Sataric, M. *Cryst. Struct. Commun.* **1980**, *9*, 473.
(20) Addison, C. C.; Greenwood, A. J.; Haley, M. J.; Logan, N. *J. Chem. Soc., Chem. Commun.* **1978**, 580.
(21) Spedding, F. H.; Derer, J. L.; Mohs, M. A.; Rard, J. A. *J. Chem. Eng. Data* **1976**, *21*, 474.
(22) Spedding, F. H.; DeKock, C. W.; Pepple, G. W.; Habenschuss, A. *J. Chem. Eng. Data* **1977**, *22*, 58.
(23) Spedding, F. H.; Rard, J. A.; Habenschuss, A. *J. Phys. Chem.* **1977**, *81*, 1069.
(24) Spedding, F. H.; Shiers, L. E.; Brown, M. E.; Derer, J. L.; Swanson, D. L.; Habenschuss, A. *J. Chem. Eng. Data* **1975**, *20*, 81.
(25) Rard, J. A.; Weber, H. O.; Spedding, F. H. *J. Chem. Eng. Data* **1977**, *22*, 187.
(26) Rard, J. A.; Shiers, L. E.; Heiser, D. J.; Spedding, F. H. *J. Chem. Eng. Data* **1977**, *22*, 337.
(27) Rard, J. A.; Miller, D. G. *J. Chem. Eng. Data* **1979**, *24*, 348.
(28) Rard, J. A.; Spedding, F. H. *J. Chem. Eng. Data* **1981**, *26*, 391.

Table I. Perchlorate Data[a]

RE	satd molality	H_2O/RE satd	H_2O/RE cryst	A_e	X	desolv ΔG, cal mol^{-1}	crystallizn energies, cal mol^{-1} ΔG	ΔH	$T\Delta S$
La	4.776	11.622	8	0.1622	0.2761	1078	3903	2137	−1766
Ce	...	...	8	...	...	1086[b]	4006[b]		
Pr	4.718	11.764	8	0.1583	0.2657	1092	4111		
Nd	4.682	11.855	8	0.1577	0.2574	1094	4251	2860	−1291
Pm	...	...	8	...	...	1094[b]	4262[b]		
Sm	4.662	11.906	8	0.1579	0.2564	1094	4272		
Eu	4.633	11.981	8	...	...	1093[b]	4324[b]		
Gd	4.622	12.010	8	0.1585	0.2494	1091	4376	3269	−1107
Tb	4.620	12.015	8	0.1567	0.2491	1098	4409		
Dy	4.604	12.056	8	0.1546	0.2497	1106	4486	4582[b]	96
Ho	4.631	11.985	8	0.1518	0.2509	1117	4451		
Er	4.622	12.009	8	0.1503	0.2494	1123	4501	5895	1394
Tm	4.622	12.009	8	0.1476	0.2491	1134	4454		
Yb	4.640	11.963	8	0.1450	0.2523	1144	4534		
Lu	4.631	11.985	8	0.1442	0.2509	1147	4572		

[a] See ref 9, 24, and 25. [b] Interpolated.

Table II. Chloride Data[a]

RE	satd molality	H_2O/RE satd	H_2O/RE cryst	A_e	X	desolv ΔG, cal mol^{-1}	crystallizn energies, cal mol^{-1} ΔG	ΔH	$T\Delta S$
La	3.894	14.253	7	0.4744	0.1379	442	3204	−870	−4074
Ce	3.90[b]	14.25[b]	7	...	...	451[b]	3270[b]	−677[b]	
Pr	3.897	14.244	7	0.4597	0.1381	460	3336	−483	−3819
Pr	...	...	6	...	...	...	...	2183	−2156[c]
Nd	3.931	14.121	6	0.4470	0.1231	477	3874	1618	−2256
Pm	3.69[c]	15.05	6	...	...	432[c]	3910[c]	...	−2350[c]
Sm	3.641	15.243	6	0.4874	0.1082	426	3936	1500	−2436
Eu	3.584	15.488	6	0.4922	0.1054	420	3985	1426	−2559
Gd	3.589	15.462	6	0.4849	0.1057	429	4058	1557	−2501
Tb	3.573	15.534	6	0.4816	0.1049	433	4132	1729	−2403
Dy	3.630	15.290	6	0.4666	0.1076	452	4196	2026	−2170
Ho	3.700	15.007	6	0.4492	0.1110	474	4271	2358	−1913
Er	3.784	14.669	6	0.4302	0.1154	500	4336	2623	−1713
Tm	3.881	14.301	6	0.4095	0.1205	529	4391	2886	−1505
Yb	4.002	13.870	6	0.3873	0.1271	562	4423	3130	−1293
Lu	4.124	13.460	6	0.3659	0.1340	597	4450	3333	−1117
Y	3.948	14.060	6	0.4017	0.1241	540	4355	2897	−1458

[a] See ref 21-23. [b] Interpolated. [c] Extrapolated.

Table III. Nitrate Data[a]

RE	satd molality	H_2O/RE satd	H_2O/RE cryst[b]	A_e	X	desolv ΔG, cal mol^{-1}	crystallizn energies, cal mol^{-1} ΔG	ΔH	$T\Delta S$
La	4.608	12.046	5 + 1	0.6080	0.1654	295	1782	−6039	−8091
Ce			5 + 1						
Pr	4.990	11.124	4 + 2	0.5535	0.1952	350	1796		
Nd	4.582	12.114	4 + 2	0.5910	0.1636	315	1805	−6062	−7967
Pm			4 + 2						
Sm	4.277	12.978	4 + 2	0.6005	0.1433	302	2108		
Eu			4 + 2						
Gd	4.370	12.702	4 + 2	0.5705	0.1492	333	2229	−5629	−7858
Tb	4.532	12.248	4 + 2	0.5481	0.1601	356	2226		
Dy	4.539	12.229	4 + 2	0.5439	0.1605	361	2248		
Ho	5.027	11.042	4 + 2	0.4904	0.1983	422	2129	−5549	−7678
Er	5.456	10.174	4 + 2	0.4416	0.2396	484	2021	−5767	−7788
Tm	5.953	9.324	4 + 2	0.3919	0.3008	555	1845		
Yb	6.650	8.347	4 + 1	0.3312	0.2988	655	2191		
Lu	6.792	8.173	4 + 1	0.3159	0.3152	683	2166	−4544	−6710

[a] See ref 21 and 26-28. [b] Inner and outer sphere; only La, Ce, and Pr determined by X-ray, others inferred.

Entropy change for crystallization is computed from the second law:

$$\Delta S_c = \Delta H_c T^{-1} - \Delta G_c T^{-1} \quad (5)$$

where the energy equivalent is $T\Delta S_c$.

Results

Pertinent data and computations for crystallization of perchlorates, chlorides, and nitrates at 298 K are listed in Tables I–III. Comprehensive data exist only for the chloride series, and yttrium chloride data are available also. Desolvation energies and ΔG_c values are plotted in Figure 1, with each rare earth given equal spacing according to atomic number. Enthalpies of crystallization are plotted in Figure 2, and entropies of crystallization are plotted in Figure 3.

Gibbs Energy Changes. The solvent structure at saturation, given by the H_2O/RE ratio and shown in Figure 4, determines both the work of removing 1 mol of water and the total work of desolvation from saturation. The water of hydration in the crystal clearly has a stronger bonding energy than the water

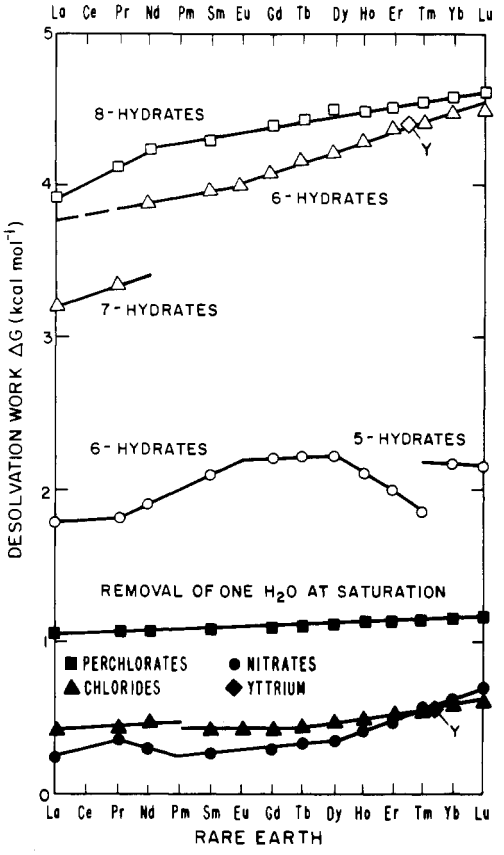

Figure 1. Gibbs energy changes on removal of 1 mol of water from saturated electrolyte and for crystallizing 1 mol of hydrate.

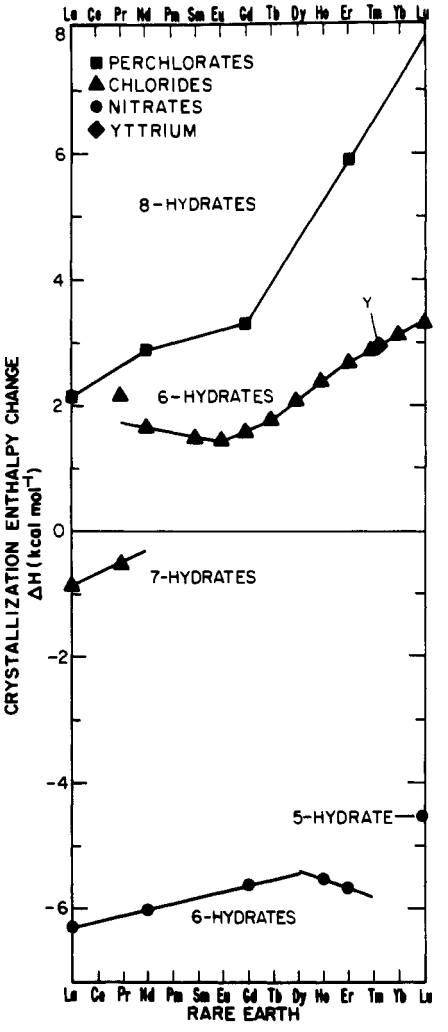

Figure 2. Enthalpy changes on crystallizing hydrates from saturated electrolytes.

removed by desolvation at saturation. In the perchlorate series the nonhydrate water is 3.62 at lanthanum, increases to 4.01 at gadolinium, and then remains constant through the rest of the series. The work of removing 1 mol of solvent water is least at lanthanum and increases gradually throughout the series. The total work of desolvation likewise increases, but the change from lanthanum to gadolinium is more pronounced than the change from gadolinium through lutetium (Figure 1). These data demonstrate an ideal series where there is predominant inner-sphere water bonding, and cation crowding is most prevalent at lanthanum. Both the desolvation energy of 1 mol of solvent water and the total desolvation energy (crystallization energy) are smooth, increasing functions. A manifestation of cation size is the solvent structure and least work of desolvation at lanthanum.

In the chloride series (Figure 1) there is a minimum of desolvation work at europium and a maximum at lutetium, but lanthanum is 22 cal mol^{-1} above europium. Occurring with this minimum is the near-maximum water content of europium electrolyte at saturation (Figure 4). Complete desolvation energies show a break at neodymium where there is a change in crystal hydrate morphology, but the plot of neodymium through lutetium shows the smooth function expected for crystallization of isostructural 6-hydrates. The work of forming 7-hydrates is about 500 cal mol^{-1} less than the work of crystallizing 6-hydrates and shows up in the difference in solvent water and the difference in electrolyte activities. The shared inner-sphere chlorides in lanthanum, cerium, and praseodymium undoubtedly also affect the crystallization energies.

Yttrium chloride falls between thulium and ytterbium according to the work of removing one solvent water (Figure 1) and also according to the enthalpy of crystallization (Figure 2), but it falls between erbium and thulium on the basis of the work of crystallization. It has the same saturated electrolyte composition as neodymium (Figure 4).

Promethium shows a pivotal position. Experimental data are needed to establish its behavior in the chloride series, as shown by Figures 1 and 4.

The nitrate series in Figure 1 shows the most variation in the work of solvent water removal. It is at a minimum at lanthanum, then increases at samarium, increases more at praseodymium, and then decreases at gadolinium. From gadolinium to lutetium it increases and more than doubles. This variation is related to the change in crystal hydrate structure between cerium and praseodymium and between thulium and lutetium where the nitrate bonding is bidentate and inner sphere. The ratio of H_2O/RE in the saturated electrolyte is greatest at samarium (or promethium) where the most solvent must be removed.

The work of crystallization of the nitrates varies considerably also. As with perchlorates and chlorides, it is at a minimum at lanthanum, but there is a second minimum at thulium that has the last (inferred) 4 + 2 inner, outer-sphere hydrate structure. The maximum occurs at dysprosium from a combination of solvent water structure and water activity. A striking effect is shown by the differences between lanthanum and praseodymium in solvent structure and crystal structure that are compensated by the differences in saturated electrolyte water activity to give essentially the same work of crystallization. The work of crystallizing nitrates is a factor of about 2 less than the work for chlorides and perchlorates.

Enthalpies of Crystallization. Tables I–III list enthalpy changes from data on heats of solution and heats of dilution for perchlorates,[9] chlorides,[22,23] and nitrates.[21] These are

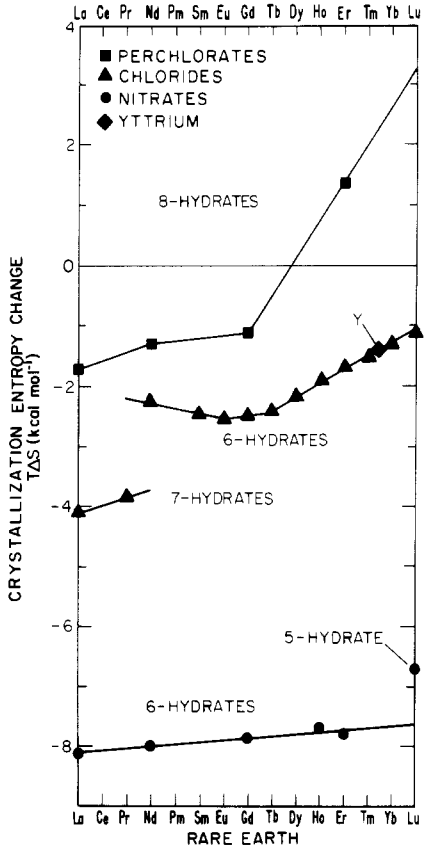

Figure 3. Entropy changes on crystallizing hydrates from saturated electrolytes.

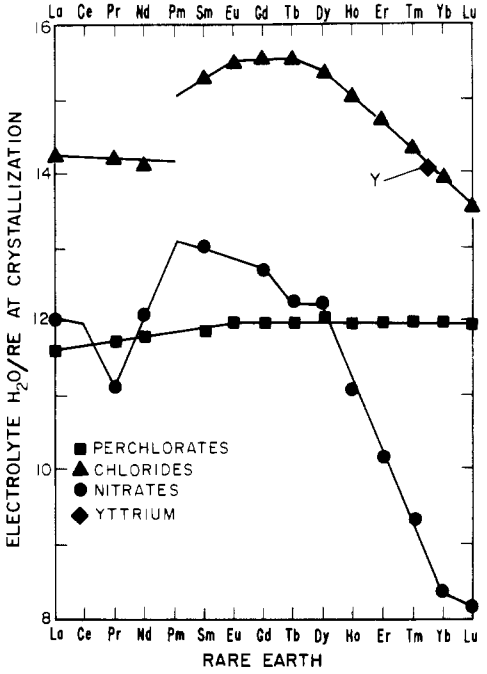

Figure 4. Composition of saturated electrolytes at the start of crystal hydrate formation.

plotted in Figure 4. The zero crossing in Figure 4 in the chloride series is associated with the change in the crystal structure and the change in the inner-sphere coordination number at praseodymium. The measured heat for the unstable $[PrCl_2(H_2O)_6]_2Cl_2$ is greater than the extrapolated value by the amount of heat evolved by the stable hydrate $[Pr_2Cl_2(H_2O)_{14}]Cl_4$.

Entropy Changes on Crystallization. Second-law values of $T\Delta S$ are listed in Tables I–III and are plotted in Figure 3. These individual values are the sum of the entropy changes associated with the phase transfer of each rare earth at saturation. These include crystal geometry effects, electrolyte structure effects, inner-sphere and outer-sphere water bonding, and inner-sphere and outer-sphere ion pairing.

Discussion

Quite striking is the near-zero formation of $T\Delta S$ for $Dy(ClO_4)_3 \cdot 8H_2O$ formation in Figure 3. We interpret this behavior to indicate a minimum in the geometric rearrangement needed for the phase-transfer reaction. The best fit of cations, anions, and water exists in both phases, and there is no change in inner-sphere water bonding. Dysprosium(III) is the cation with near-optimum size to match the geometry of the perchlorate anion structure and solvent water when crystallization in the saturated electrolyte starts.

The negative entropy change in the perchlorate series can be interpreted to show the effect of cation crowding from lanthanum to dysprosium, and the positive change may show the effect of anion crowding from dysprosium through lutetium. There is the additional possibility of a cation coordination number decrease in the saturated electrolyte somewhere in the series.[29,30] If the negative entropy change is due to more order in the crystalline hydrate phase, then the positive entropy change in the rare-earth perchlorates can be explained by more disorder in the crystal hydrate compared to the saturated electrolyte. With anion crowding there seems to be a more rigid anion structure in the electrolyte, and the inner-sphere cation water is not squeezed.

In the chloride series between praseodymium and neodymium a large change occurs in the crystal morphology and composition resulting from change in the cation size. On going from praseodymium to neodymium, two inner-sphere waters are lost, two inner-sphere shared chlorides are replaced by four inner-sphere chlorides, and the dimeric morphology is retained by substituting hydrogen bonding for chloride bridge bonding. The crystal cation coordination number changes from 9 to 8. From Figure 3, this overall effect is, by back-extrapolation of neodymium to praseodymium, 1600 cal mol^{-1} at praseodymium. The difference by extrapolation at neodymium is 1450 cal mol^{-1}. Thus, the geometric cation stabilization energy for the chloride-bridged structure is about 150 cal mol^{-1} at praseodymium by the extrapolation procedure.

Another effect of cation size is shown by $Lu(NO_3)_3 \cdot 5H_2O$, if the extrapolation in Figure 3 is valid. Here the extrapolated change in $T\Delta S$ is 900 cal mol^{-1}, but there is no crystal information to detail structural differences among lutetium, ytterbium, and thulium. Lutetium may show a smaller coordination number.

The negative $T\Delta S$ slope between neodymium and europium chlorides could be an indication of worsening ion fit with increasing atomic numbers and may show the effect of cation size on changing the cation coordination number in the electrolyte phase. The electrolyte structure at saturation between neodymium and europium changes by an increase of 1.4 waters as shown in Table II and Figure 4. Maximum solubility is shown by neodymium, and the triad europium, gadolinium, and terbium shows minimum solubility. Habenschuss and Spedding assigned electrolyte cation coordination numbers of 9 for lanthanum, praseodymium, and neodymium and 8 for heavier rare earths on the basis of X-ray diffraction studies of concentrated chloride solutions.[29] They suggested that a change in coordination number takes place between neodymium and europium in the chloride series. Neutron diffraction measurements by Narten and Hahn showed 8.5 inner-sphere

(29) Habenschuss, A.; Spedding, F. H. *J. Chem. Phys.* **1979**, *70*, 2797, 3758.
(30) Narten, A. H.; Hahn, R. L. *Science (Washington, D.C.)* **1982**, *217*, 1249.

waters for neodymium at molality 2.89,[30] but this number could change at the saturation molality of 3.93 where the electrolyte accommodates 5.1 less waters per neodymium.

The 6-hydrate nitrate series shows no abrupt changes in the $T\Delta S$ slope in Figure 3 that can be attributed to inner-sphere-bonding changes. However, data on all of the rare earths are needed to verify this conclusion. The large negative entropy change for each rare earth seems to be a result of moving nitrates inner sphere and removing inner-sphere water when the crystal is formed. Nitrate ion can penetrate the inner-sphere water structure and occupy two coordinate positions. The maximum number of inner-sphere nitrate positions is 10 for Ce(III),[31] Ho(III),[32] and Y(III)[20] when there is no inner-sphere water. In an analogous Sc(III) compound, only nine coordinate positions exist, with eight being bidentate and one monodentate.[20] The number of nitrates that will displace inner-sphere waters will depend not only on electrolyte and crystal compositions but also on cation size. Structural data are needed to determine whether the inner-sphere water in $Lu(NO_3)_2 \cdot 5H_2O$ is one less than the other rare-earth cations.

We are unable at this time to make a complete assessment because of insufficient data. Solubility data and water activity data are needed for promethium chloride and nitrate electrolytes to establish the trend in crystallization behavior. Additional data are needed for the perchlorate series to establish $T\Delta S$ desolvation changes. Crystal structure determinations are needed for the perchlorate and nitrate series for evaluation of the desolvation mechanisms at saturation. Data for cerium and europium electrolytes are generally lacking.

In a following paper we calculate the energy requirements for desolvation of rare-earth perchlorates, chlorides, and nitrates from 0.1 m to saturation. We apply the second law for partial molal and integral changes.

Acknowledgment. The authors thank R. J. Bard, M. G. Bowman, and L. B. Asprey for discussions that helped considerably in writing this paper. We thank the U.S. Department of Energy, Office of Basic Energy Sciences, Division of Chemical Sciences, for support.

Registry No. $[Pr_2Cl_2(H_2O)_{14}]Cl_4$, 67573-46-0; $[PrCl_2(H_2O)_6]_2Cl_2$, 90432-19-2; $[NdCl_2(H_2O)_6]_2Cl_2$, 90432-20-5; $[Pr(NO_3)_3(H_2O)_4] \cdot 2H_2O$, 59964-37-3; $Dy(ClO_4)_3 \cdot 8H_2O$, 90432-21-6; $Lu(NO_3)_3 \cdot 5H_2O$, 34767-08-3.

(31) Al-Karaghouli, A.; Wood, J. S. *J. Chem. Soc., Dalton Trans.* **1973**, 2318.
(32) Toogood, E.; Chieh, C. *Can. J. Chem.* **1975**, *53*, 831.

Contribution from the Departments of Chemistry, University of Michigan, Ann Arbor, Michigan 48109, and University of Chicago, Chicago, Illinois 60637

Electronic Switching of Ring Orientation in Cyclopentadienyl-Bridged Polymers

ENRIC CANADELL,*[1a,b] ODILE EISENSTEIN,*[1a,c] and TIMOTHY HUGHBANKS*[1d]

Received December 1, 1983

The electronic and structural properties of cyclopentadienyl-bridged polymers $(Cp_2Pb)_n$ and $(CH_3ZnCp)_n$ are studied with a tight-binding method of band structure calculation. The orientation of the bridging cyclopentadienyl is related to the number of valence electrons at the metal center. In $(Cp_2Pb)_n$, the structure minimizes the antibonding interaction between the Pb and the bridging Cp occupied orbitals. In contrast, in $(CH_3ZnCp)_n$, which has two electrons less per metal center, the structure maximizes the bonding interaction between the empty Zn and the occupied Cp orbitals. The structural characteristics of $(Cp_2Mn)_n$ are discussed. New types of polymers are suggested.

Since the discovery of ferrocene, dicyclopentadienyl complexes Cp_2M have come to form a large class of molecules.[2] Most of the complexes are monomeric in the gas phase and the solid state. Their structural and electronic properties have been extensively studied. The species Cp_2Pb[3] polymerizes in the solid state as does a related species, $CpZnCH_3$.[4] Both of these systems are characterized as consisting of one-dimensional zigzag chains of metal atoms separated by bridging cyclopentadienyl ligands. Of particular interest is the orientation of the bridging cyclopentadienyl. In $(Cp_2Pb)_n$ (**1**) the

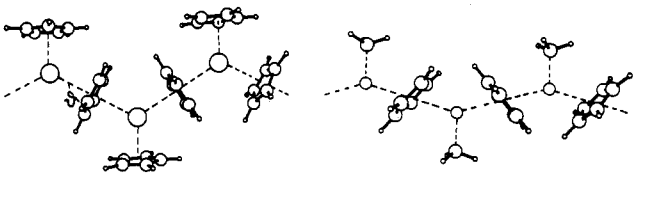

1 2

bridging cyclopentadienyl is perpendicular to the vector joining adjacent Pb centers as if to coordinate each Pb in a η^5 fashion. An additional cyclopentadienyl ligand caps the metal in a η^5 fashion to complete the Pb coordination sphere. In $CpZnCH_3$ (**2**) the bridging cyclopentadienyl is inclined with respect to the Zn–Zn vector.[4] In this orientation the cyclopentadienyl rings appear to become η^2 with respect to one metal center and η^3 with respect to the other.

A compound with obvious structural similarities to the above systems is Cp_2Mn,[5] which polymerizes to form the structure

(1) (a) University of Michigan. (b) Present address: Department of Chemistry, University of Chicago. (c) Present address: Laboratoire de Chimie Theorique Batiment 490, Universitê de Paris-Sud, 91405 Orsay, France. (d) University of Chicago.
(2) For non transition metals: (a) Cp_2Pb: Almenningen, A.; Haaland, A.; Motzfeldt, T. *J. Organomet. Chem.* **1967**, *7*, 97. (b) Cp_2Ca: Zerger, R.; Stucky, G. *Ibid.* **1974**, *80*, 7. Diindenylmagnesium: Atwood, J. L.; Smith, K. D. *J. Am. Chem. Soc.* **1974**, *96*, 994. (c) $(Me_2Cp)_2M$ (M = Ge, Sn, Pb): Bonny, A.; McMaster, A. D.; Stobart, S. R. *Inorg. Chem.* **1978**, *17*, 935. Atwood, J. L.; Hunter, W. E.; Cowley, A. H.; Jones, R. A.; Stewart, C. A. *J. Chem. Soc., Chem. Commun.* **1981**, 925. Baxter, S. G.; Cowley, A. H.; Lasch, J. G.; Lattman, M.; Sharum, W. P.; Stewart, C. A. *J. Am. Chem. Soc.* **1982**, *104*, 4064. Almlöf, J.; Fernholt, L.; Faegri, K., Jr.; Haaland, A.; Schilling, B. E. R.; Seip, R.; Taugbøl, K. *Acta Chem. Scand., Ser. A* **1983**, *A37*, 131. (d) Jutzi, P.; Kohl, F.; Hofmann, P.; Krüger, C.; Tsay, Y.-H. *Chem. Ber.* **1980**, *113*, 757. (e) Cp_2As^+: Baxter, S. G.; Cowley, A. H.; Mehrotra, S. K. *J. Am. Chem. Soc.* **1981**, *103*, 5572. (f) For the large subject of transition-metal metallocenes see, for instance, a review article by: Haaland, A. *Acc. Chem. Res.* **1979**, *12*, 415.
(3) Panattoni, C.; Bombieri, G.; Croatto, U. *Acta Crystallogr.* **1966**, *21*, 823.
(4) Aoyagi, T.; Shearer, H. M. M.; Wade, K.; Whitehead, G. *J. Organomet. Chem.* **1978**, *146*, C29. $CpZnCH_3$ monomeric: Haaland, A.; Samdal, S.; Seip, R. *Ibid.* **1978**, *153*, 187.
(5) Bünder, W.; Weiss, E. *Z. Naturforsch., B: Anorg. Chem., Org. Chem.* **1978**, *33B*, 1235.

0020-1669/84/1323-2435$01.50/0